NUMERICAL SIMULATION OF DROPLET BREAKUP, SPLITTING AND SORTING IN MICROFLUIDIC DEVICE

T. Chekifi, B. Dennai, R. Khelfaoui

University Tahri Mohammed Bechar Bechar
Laboratory ENERGARID
Bechar, Algeria
chekifi.tawfiq@gmail.com

Accepted October 19, 2015

Abstract

Droplet in microfluidic is applied to lab-on-a-chip devices for biomedical testing and synthesis, droplets of water–in-oil are produced by flow focusing technique; an obstacle configuration is used to split the droplet. The finite volume numerical method was applied to solve the Navier–Stokes equations in conjunction with the Volume of Fluid (VOF) approach for interface tracking of the commercial code FLUENT. Numerical simulations were carried out for different flow conditions. The effects of some parameters on the droplet motion were investigated to find the optimal conditions for droplet breakup. The numerical results show that the main channel width, the surface tension, the contact angle and the capillary number of continuous phase play an important role on the droplet generation. The computation also demonstrates that an obstacle configuration can be used to split droplet, where the latter are sorted in the end of the main channel. It also demonstrates that the volume of fluid method is an effective way to simulate the generation of droplets in flow focusing configuration.

Nomenclature

f: frequency (Hz)
u: velocity (m / s)
u_c: continuous phase velocity (m / s)
u_d: dispersed phase velocity (m / s)
n: unit vector normal to the interface
κ: curvature of the interface
F: the surface tension force
W: width (mm)
ρ: density (kg / m^3)
μ: dynamic viscosity (kg / m · s)
α: phase fraction (%)
σ: the surface tension coefficient (N / m)
τ: time (s)
W: width of the main channel
W_c: width of continuous phase inlet
W_d: width of continuous phase inlet
ρ_c: continuous phase density
ρ_d: dispersed phase density

1. Introduction

Over the last few decades, modeling immiscible fluids such as oil and water have been a classical research topic. Droplet-based microfluidics presents a unique platform for mixing, reaction, separation, dispersion of drops and numerous other functions [1, 2]. Droplet-based

microfluidics is of great interest for biological research, chemical synthesis, drug delivery and medical diagnostics.

Droplet-based microfluidics refers to devices and methods for controlling the fluid flows in length scales smaller than one millimeter. Monodisperse droplets in microfluidic devices have been generated using different microchannel configurations such as T-junction [3, 4], flow focusing [5], or co-flowing [6]. In microfluidics, controlling droplet size is a core technique not only for producing highly monodisperse emulsions [7], but also for using the droplet itself as a tool for manifold purposes [8, 9]. As for droplet breakup, Link et al. introduced two methods to reduce droplet size using T-junction or a square obstruction deposited in the center of the channel [10]. As these methods are passive ways in droplet manipulation, it provides a way of reducing droplet size in a rapid process with a narrow size distribution. As this is an effective process to reduce the droplet size, it is worthwhile to get physical insights through numerical analysis on the relevant droplet flows in microfluidics [11].

In recent studies, unlike relatively simple geometries such as T-junctions [12, 13] or flow focusing devices [14, 15], novel designs have been developed for improved manipulation of droplets. Lee et al. [16] presented a one-step method for size control and sorting of droplets in a modified flow focusing geometry with a moving wall technique operated by pressure inlets. Also, in a cross-shaped channel, droplet generation by a thread breakup due to pressure inlets at both sides was shown with a surface treatment technique [17]. Droplet fusion devices were also proposed using a hydrodynamic trap at a wide cross channel [18, 19], at a tapered channel [20], at a fluid resistance in straight channels [21], and an array of pillar elements [22]. As mentioned previously, an obstruction in microchannel can also be utilized to reduce the droplet size [10]. Menech [23] was performed numerical analysis to figure out the droplet breakup process and optimize the geometry configuration for the process. In which, the author suggested T-junction channel using a phase-field method to compute droplet breakup, Carlson et al. [24] extended the phase field method to simulation of droplet motion in a Y-junction channel. Their results showed that the tip of the junction affected the droplet deformation, and the droplet breakup or non-breakup regime depended on the capillary number and droplet size. The droplet breakup by a circular cylinder in a microchannel was computed by Chung et al. [25] using a front tracking method, in which the droplet shape was represented by the moving front elements. Their numerical results showed that the split droplets merged in the rear side of the obstacle when the capillary number was not large.

Although various studies on the generation of droplets in T-junction and flow focusing devices have been carried out, a fundamental understanding of the flow physics that account for the effect of the geometry of the devices is still missing. In addition, simulation of two immiscible phases flow in complex geometry is a challenging work [26].

Computational fluid dynamics (CFD) studies allow for broad parametric variations that are hard to study experimentally. CFD also provides detailed information on flow details such as pressures and velocities that are difficult to measure experimentally, and can thus provide mechanistic insights needed to check various hypotheses. Recently, the volume of fluids method has been proved to be a powerful method to simulate droplet dynamics [27]. In this method, the interface is given implicitly by a color function, which is defined as the volume fraction of one of the fluids within each cell. From this function, a reconstruction of the interface is made and the interface is then propagated implicitly by updating the color function. VOF methods are conservative and can deal with topological changes of the interface. However,

VOF methods cannot accurately compute several important properties, such as curvature and the normal to the interface. Moreover, a high order of accuracy is hard to achieve because of the discontinuities in the color function [27].

Motivated by the previous work [26] and [28], using a VOF method, we perform a two-dimensional numerical CFD study of droplet breakup, splitting and sorting, in the present study we suggest device that allows droplet breakup in flow focusing configuration, splitting and sorting. In this microsystem, the effect of main channel size and capillary number on the droplet dynamics is investigated. In previous numerical works [26, 29, 30], surface tension plays a significant role on the droplet deformation in confined microchannel flows. In the same manner, by testing a several values between both phases, we expect that this parameter affects the droplet dispersion in the microchannel. In which, the effects of inertia and gravity in the volume does not play an important role with respect to the macroscopic scale. We also study the droplet breakup as function of the capillary number and the main channel size to find the optimal conditions for droplet detachment. In our model, we investigate the droplet splitting and sorting by size in the end of the main channel by the use of an obstacle. The frequency of droplet generation and droplet sorting is also considered. Finally, we suggest useful ideas for manipulating droplets in microchannel flows.

2. Description of the system and geometries

The physics to be simulated involves droplet breakup by flow focusing technique. Three sizes of the main channel are evaluated to produce water-in-oil droplet. There are two oil inlets, one water inlet and one outlet in. All the micro- channels are 5 mm long. The description of the geometries is presented in **Figure 1**. Due to the existence of the obstacle, two sub-channels are formed in the end of main channel.

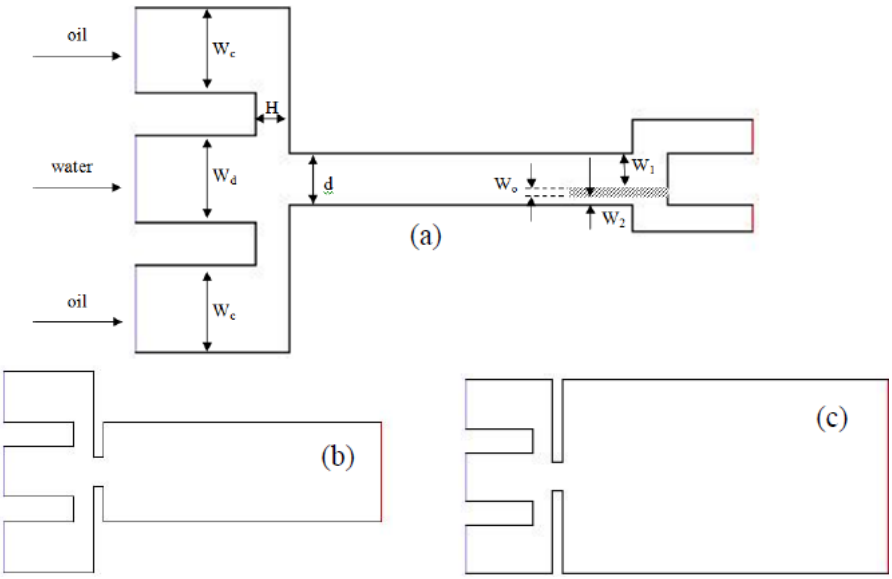

Figure 1. (a): Schematic of flow focusing configuration. $W_c = W_d = 2$. An orifice with width d = 1.2 is placed at a distance H = 0.8 downstream of three coaxial streams. The main channel width is varied (a): W = 1.2, (b): W = 4 and (c): W = 8). $W_o = 0.16$, sub-channel1: $W_1 = 0.8$, sub-channel 2:$W_2 = 0.24$. The total length of the configuration is 12. (All the numbers are in mm).

In our system, the droplet is generated by the flow focusing, which has been widely used for generating highly spherical droplet [31 – 33]. **Figure 1** shows the flow focusing geometry implemented into a microfluidic device. In this structure, the dispersed phase flows in the middle of the channel, while the continuous phase flows through upper and lower channels. The continuous phase and dispersed phase penetrate into the downstream channel, and the continuous phase exerts pressure and stress which force the dispersed phase into a narrow thread. The dispersed phase breaks inside or downstream of the orifice, then the droplet is generated at the end of the flow stream where the neck forms.

The surface tension term reflects the interfacial force between the discrete liquid (droplet) and the continuous liquid. The interaction (attraction or repulsion) between droplets results from the continuous liquid flow which is affected by the interfacial forces existing at each droplet surface.

3. Numerical approach

The segregated solver for an unsteady laminar flow was used in CFD, the volume of fluid method was performed to track the interface between water droplet and the continuous phase. The VOF model is a surface-tracking technique that is useful when studying the position of the interface between two immiscible fluids. A single set of momentum equations is shared by the fluids, and the volume fraction of each of the fluids in each computational cell is tracked throughout the domain. The VOF model uses phase averaging to define the amount of continuous and dispersed phase in each cell. A variable, α, was defined as [29, 30]:

$\alpha = 1 \Rightarrow$ when the cell is 100 % filled with continuous phase

$\alpha = 0 \Rightarrow$ when the cell is 100 % filled with dispersed phase

$0 < \alpha < 1 \Rightarrow$ when the cell contains an interface between the two phases

The density ρ, and viscosity μ, for both phases (water and oil) can be calculated using a linear dependence:

The subscript 1 is chosen for the continuous liquid (primary) phase, while the subscript 2 for the discrete phase (microdrops)

$$\rho = \rho_1 \alpha + \rho_2 (1 - \alpha), \quad (1)$$

$$\mu = \mu_1 \alpha + \mu_2 (1 - \alpha). \quad (2)$$

There are several different VOF algorithms with different accuracies and complexities in CFD. The geometric reconstruction scheme used in this study is based on the work of Youngs (1982) [33] and further described by Rudman (1997) [34]. This scheme permits a piecewise-linear approach, which assumes that the interface has a linear slope within each cell, and the position of the interface is calculated from the volume fraction and their derivatives in the cell. The solutions of the velocity field and pressure are calculated using a body-force-weighted discretization scheme for the pressure, the Pressure-Implicit with Splitting of Operators (PISO) scheme for the pressure velocity.

The body-force-weighted scheme is used since it works well with the VOF model, and the PISO scheme is chosen to improve the efficiency of the calculation of the momentum balance after the pressure correction equation is solved. The CFD software was used to simulate the flow of oil microdrops sorting. The governing equations are the mass conservation equation for each phase and the momentum equation:

$$\partial_t C + \vec{u} \nabla C = 0, \quad (3)$$

where the velocity is given by u. In addition, a single momentum equation is used for the mixture of two-phase-fluid.

The momentum equation hence is described by

$$\partial_t(\rho u) + \nabla \cdot (\rho u u) + \nabla u \cdot \nabla[\mu] = -\nabla P + F , \quad (4)$$

where F is the surface tension $F = \sigma(x)n$ force, P is the curvature of the interface and n is a unit vector normal to the interface. σ is the surface tension coefficient.

4. Droplet simulation and parameters

FLUENT 6.3 in CFD software was used to model droplet formation in the microfluidic by flow focusing configuration (see **Figure 1**). The volume of fluid (VOF) model in three-dimensional form was used, which enables capturing and tracking the precise location of the interface between the fluids. The VOF method operates under the principle that the two or more fluids are not interpenetrating. The flows are taken to be two-dimensional and laminar. In the simulations, a constant velocity boundary scheme proposed by Zou & He [32] is imposed on both water and oil inlet and the pressure of outlet is the same as the atmospheric pressure. At the position where the fluid meets the solid walls, half-way bounce-back boundary scheme is applied to achieve the non-slip velocity condition at the solid walls. The viscosities of both liquids water and gasoil are respectively defined as $\mu_w = 0.001$ and $\mu_o = 0.003$ kg / m · s. An equilibrium contact angle $\theta = 60°$ were prescribed. This contact angle is used to correct the surface normal in the vicinity of the wall, and therefore adjusts the curvature of the interface and the surface tension calculation near the wall [35]. The second-order upwind scheme is used for discretization of the momentum equation. The PISO scheme is taken as the pressure-velocity coupling scheme, while the PRESTO! is taken as the pressure discretization scheme. The geometric reconstruction scheme is used for interpolation of the interface geometry. It is able to form mono-dispersed droplets by this way due to the different surface tensions of two fluids.

The computations were run for a large number of time steps (10^{-5}) to generate a database from which statistically converged mean and perturbation flow quantities could be extracted. The convergence limit was set to a residual sum of 10^{-3} for the continuity and velocity components. These results are discussed in the following sections.

The requirement to successfully follow of droplets behavior leads to very large numbers of grid cells when uniform meshes are used. Three intervals mesh sizes were tested to obtain grid independent solutions (h = 0.06, 0.08 and 0.10 μm). The relative difference of droplet volumes and interface shapes between successive mesh sizes is observed to be small as the mesh size decreases. Therefore, our simulations in this study are done with $h = 1$ μm to save computing time without losing the accuracy of the numerical results.

4.1. The main channel width effects

To test whether the confinement of geometry plays an important role in the breakup of plugs, we first perform computations to investigate the effect of the main channel width on the droplet flow regime. In the simulations, to single out the geometrical parameter, the inlet flow velocity of both phases is ($u_d = u_c = 0.2$ m / s), the densities of both fluids are $\rho_c = 830$ and $\rho_d = 998.2$ kg / m^3. the results for three configuration are presented in the **Figure 2**.

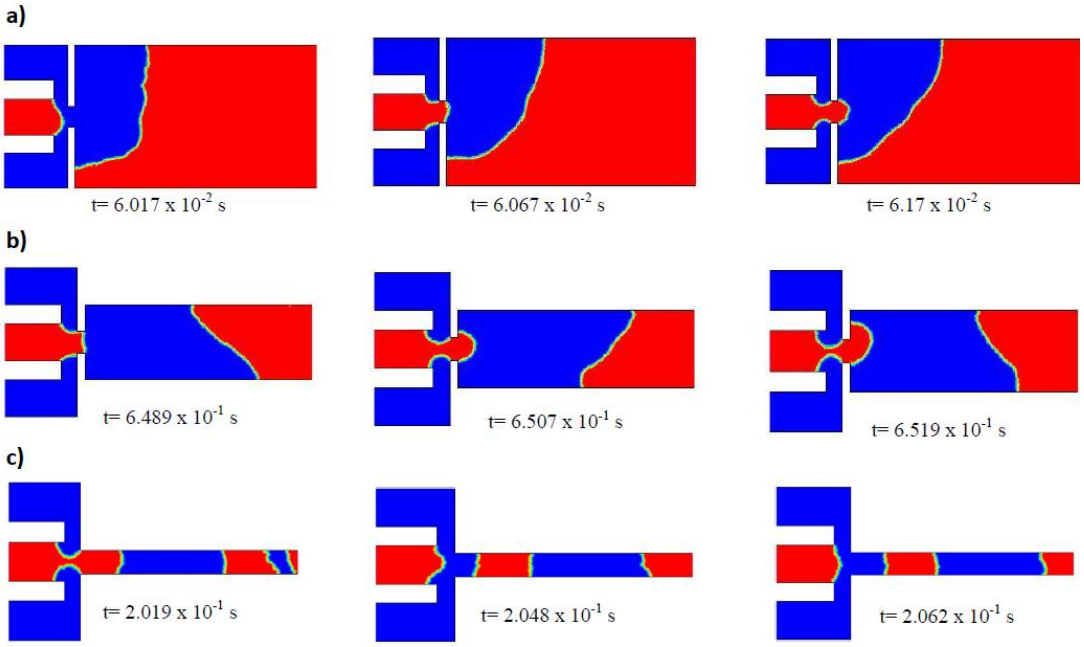

Figure 2. The droplet generation at $u_d / u_c = 1$ ($u_d = u_c = 0.2$ m / s) for three different widths of main channel. (a) W=8mm, b) W=4mm and c) W=1.2mm.

The geometry effect, i.e., the width of the main channel (W) plays an important role in the flow dispersion in the main channel **Figure 2**, at the same conditions for large main channel the flow is observed in thread regime due to the accumulation of generated droplets, which are flew with low velocity **Figures 2a** and **b**, where droplet emerging is occurred. For the smallest model **Figure 2c**, no emerging is observed, because droplets flow with high velocities. Therefore, the flow pattern is clearly observed with high dispersion. For the next sections, we use the smallest model with main channel width = 1.2 mm.

4.2. Surface tension effect

For two phase flows in microchannels, the surface tension forces play an important role in determining the dynamics of droplets, whereas gravitational forces are generally less important, we investigate the influence of surface tension coefficient on the droplet flow regime.

In this subsection, we use water as the dispersed phase and oil as the continuous phase, and observe flow regime, which depends on the surface tension coefficient. The densities of the continuous and dispersed phase are assumed respectively $\rho_c = 830$ and $\rho_d = 998.2$ kg / m^3. The channel surface is hydrophobic, i.e., the contact angle between dispersed phase and the channel surface is $\theta = 0°$. It is shown in **Figure 3** that for capillary numbers which define flows in the jetting to dripping regime through numerical simulations, and quantify the results in terms of the "stable" droplet formation regime in a microchannel. for a given inlet velocity of both phases ($u = 0.2$ m / s) As shown in **Figure 3**, three typical flow patterns are identified for different surface tension at a fixed capillary number ($Ca = 3.43 \cdot 10^{-2}$). For low σ, thread regime of dispersed phase is clearly observed, as we increase σ, the thread becomes unstable after a distance of laminar flow $\sigma = 0.01$ N / m, for higher surface tension $\sigma = 20$ N / m, droplet are formed with high dispersion due to the squeezing mechanism. For the next simulations, we use σ=20N/m to generate mono dispersed droplet.

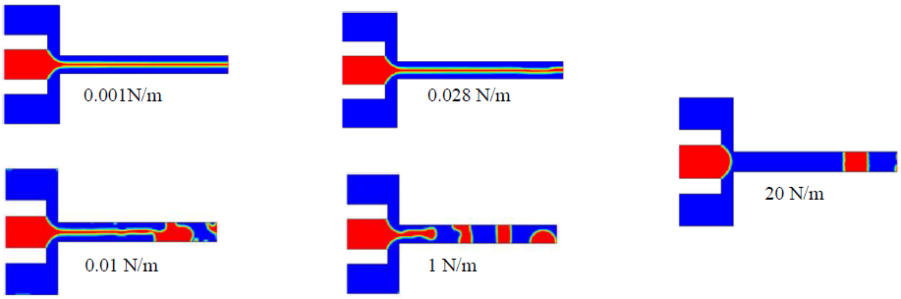

Figure 3. Droplet flow regimes as a function of the surface tension (σ) for u_c / u_d=1 ($u_c = u_d$ = 0.2 m / s) for the small model.

4.3. Contact angle effect

Wetting properties are usually characterized by the contact angle on a surface. Young's law provides the relation between interfacial tensions and contact angle. For a water droplet on a surface, surrounded by oil, the equilibrium contact angle is [36]:

$$\cos(\theta) = \frac{\sigma_{oil.wall} - \sigma_{water.wall}}{\sigma_{oil.water}}.$$

where $\sigma_{oil,wall}$ is the interfacial tension of oil with the wall surface, water, wall is the interfacial tension of water with the wall surface, and $\sigma_{oil,water}$ is the interfacial tension of the oil with water.

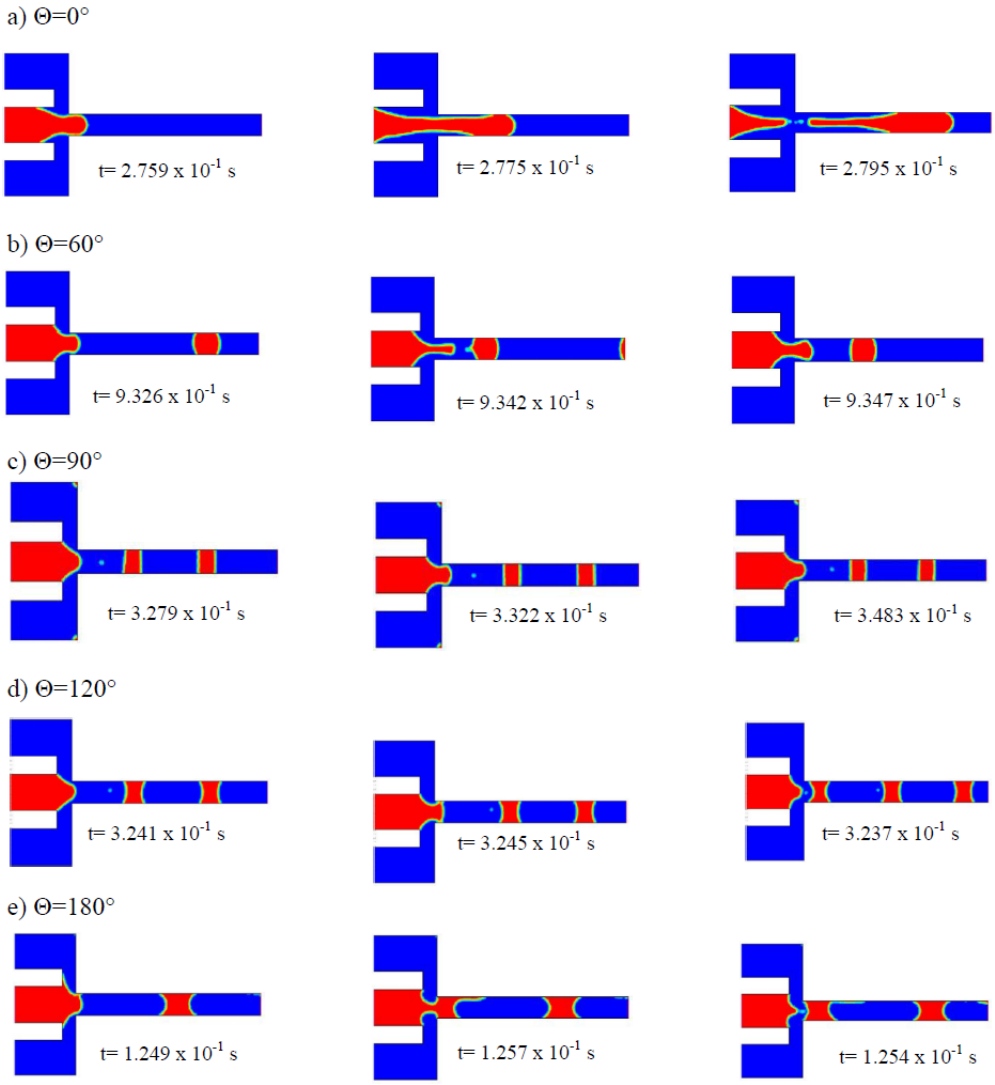

Figure 4. Droplet (water-in-oil) flow pattern as a function of contact angle at Ca = 0.053 (u_c = 0.5 m / s and u_d = 0.3 m / s) and σ = 10 N / m.

A constant contact angle associated to a non slip condition was imposed at the contact point between the gas–liquid interface and the walls defining our structure. The corresponding numerical procedure is described in detail in Dupont and Legendre [20]. The result of the droplet flow pattern as function of contact angle is presented in the **Figure 4**.

The wetting properties of the fluids relative to the channel walls, more specifically the contact angle, have also been shown to affect the two-phase flow patterns in microchannels [41]. In order to determine the influence of the contact angles on droplet shape, different values of the contact angles (Θ = 0, 60, 90, 120 and 180 °) are tested by keeping the same conditions to find the optimum contact angle to obtain spherical form of droplet. It is clearly observed that the droplet takes a shape for each contact angle. For Θ = 0 °, elongated droplet are observed with low production frequency, whereas the rest of contact angle the geometrical form is smaller. For Θ = 90 °, the droplet takes uniform rectangular shape with high production frequency compared of Θ = 0 °. For both Θ = 120 ° and Θ = 180 ° droplets take concaved shape in its extremity. The contact angle of 60 ° is the optimum condition for droplet flow pattern; which is used for the next sections. The droplet are taken uniform spherical shape.

5. Droplet splitting and sorting

Numerical simulations of droplet breakup and splitting are performed using VOF method, droplet of water-in-oil are generated by flow focusing configuration, The simplest droplet sorting techniques require no detection or switching mechanisms, but instead rely on creative device geometry that allows the separation of droplets by size. By simply creating an obstacle geometry in which the daughter channels had different widths, droplets were induced to sort into one of the channels (**Figure 5**). The split daughter droplets pass the sub-channels, while the bigger split daughter droplets pass the sub-channels 2. When a droplet collides with the obstacle, it splits into the obstacle-wall gaps (or sub-channels). The split portions of droplet leave out the sub-channels to the outlet of microsystem.

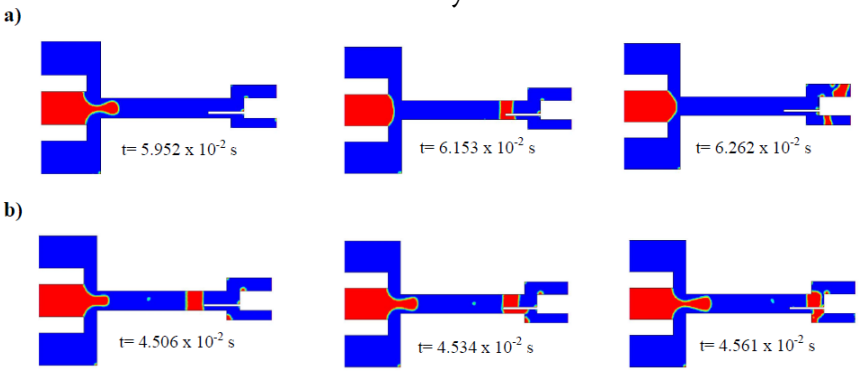

Figure 5. Droplet breakup, splitting and sorting for two different capillary numbers: a) u_c =1 m / s, u_d = 0.1 m / s, Ca = $5.36 \cdot 10^{-2}$ and b) u_c = 0.5 m / s, u_d = 0.3 m / s, Ca = $6.64 \cdot 10^{-2}$.

Figure 5 shows the droplet motion. A convergence test for grid resolutions is first conducted for droplet breakup by the use of a quadrate obstacle. Water-in-oil droplet are generated by flow focusing configuration, splitting of droplet is performed by thinner obstacle at the end of the main channel, for both capillary numbers (Ca = $5.36 \cdot 10^{-2}$ and $6.64 \cdot 10^{-2}$). We observe for in three successive moments that the split daughter droplets pass the sub-channels without re-merging unlike; our numerical simulations are in good agreement with previous works of [2] and [37]. It is also seen from **Figure 5b** that the droplet volume fraction is higher for higher capillary number **Figure 4b**, as we demonstrated in the previous section. Due to

difference of both sub-channel widths, the bigger split daughter droplets pass the sub-channels 1, while the smaller split daughter droplets pass the sub-channels 2.

The present computations demonstrate that an inclined obstacle can be used as an effective method for droplet splitting with even-sized daughter droplets.

6. Conclusions

Droplet generation in flow focusing configuration, splitting and sorting were investigated numerically by using the VOF method of the commercial code FLUENT. Various parameters which affect the generation of the droplets, including capillary number, geometry of configuration, surface tension and contact angle are systematically analyzed. It shows that the droplet breakup depends on fluid properties such as capillary number, surface tension and the main channel width. We also find that the flow focusing configuration with the smaller main channel width likely to generate stable droplet. The capillary number is an important parameter to define the droplet length and droplet generation frequency. The increase of this parameter leads to the increase of droplet frequency, while it conducts to small droplet length. The numerical simulations of droplet breakup also showed that the obstacle configuration is effective for droplet splitting and sorting, where, daughter split droplet are sorted into smaller droplet that passed through small sub-channel and the bigger passed the bigger sub-channel.
We hope this numerical study helps understanding the underlying physics on the droplet dynamics as well as designing the complicated flows in future microfluidic applications.

Acknowledgment

The authors wish to acknowledge ENERGARID laboratory, especially the group of integral system control.

References

1. M. A. Burns, C. H. Mastrangelo, T. S. Sammarco, F. P. Man, J. R. Webster, B. N. Johnson, B. Foerster, D. Jones, Y. Fields, A. R. Kaiser, D. T. Burke. Microfabricated structures for integrated DNA analysis. Proc. Natl. Acad. Sci. USA, 1996, 93, 11, 5556-5561.
2. U. Lehmann, S. Hadjidj, V. K. Parashar, C. Vandevyver, A. Rida, M. A. M. Gijs. Two-dimensional magnetic manipulation of microdroplets on a chip as a platform for bioanalytical applications. Sens. & Actuat. B, 2006, 117, 2, 457-463.
3. P. Garstecki, M. J. Fuerstman, H. A. Stone, G. M. Whitesides. Formation of droplets and bubbles in a microfluidic T-junction – Scaling and mechanism of break-up. Lab Chip,,2006, 6, 3, 437- 446.
4. J. H. Xu, S. W. Li, J. Tán, Y. J. Wang, G. S. Luo. Preparation of highly monodisperse droplet in a T-junction microfluidic device. AIChE J., 2006, 52, 9, 3005-3010.
5. N. T. Nguyen, T. H. Ting, Y. F. Yap, T. N. Wong, J. C. K. Chai, W. L. Ong, J. Zhou, S. H. Tan, L. Yobas. Thermally mediated droplet formation in microchannels. Appl. Phys. Lett., 2007, 91, 084102.
6. J. H. Xu, S. W. Li, W. J. Lan, G. S. Luo. Microfluidic approach for rapid interfacial tension measurement. Langmuir, 2008, 24, 19, 11287-11292.
7. L. Y. Chu, A. S. Utada, R. K. Shah, J. W. Kim, D. A. Weitz. Controllable monodisperse multiple emulsions. Angew. Chem. Int. Ed., 2007, 46, 8970-8974.
8. S. Y. Teh, R. Lin, L. H. Hung, A. P. Lee. Droplet microfluidics. Lab. Chip., 2008, 8, 198-220.
9. G. M. Whitesides. The origins and the future ofmicrofluidics, Nature, 2006, 442, 368-373.
10. D. R. Link, S. L. Anna, D. A. Weitz, H. A. Stone. Geometrically mediated breakup of drops in microfluidic devices. Phys. Rev. Lett., 2004, 92, 054503.
11. Ch. K. Chung, K. H. Ahn, S. J. Lee. Numerical study on the dynamics of droplet passing through a cylinder obstruction in confined microchannel flow. J. Non-Newtonian Fluid Mech., 2009, 162, 38-44.

12. T. Thorsen, R. W. Roberts, F. H. Arnold, S. R. Quake. Dynamic pattern formation in a vesicle-generating microfluidic device. Phys. Rev. Lett., 2001, 86, 4163-4166.
13. C. Priest, S. Herminghaus, R. Seemann. Generation of monodisperse gel emulsions in a microfluidic device. Appl. Phys. Lett., 2006, 88, 024106.
14. S. L. Anna, N. Bontoux, H. A. Stone. Formation of dispersions using "flowfocusing" in microchannels. Appl. Phys. Lett., 2003, 82, 364-366.
15. S. L. Anna, H. C. Mayer. Microscale tipstreaming in a microfluidic flow focusing device. Phys. Fluids, 2006, 18, 121512.
16. C.-Y. Lee, Y.-H. Lin, G.-B. Lee. A droplet-based microfludic system capable of droplet formation and manipulation. Microfluid. & Nanofluid., 2009, 6, 599-610.
17. Y. C. Su, L. W. Lin. Geometry and surface-assisted micro flow discretization. J. Micromech. & Microeng., 2006, 16, 1884-1890.
18. Y. C. Tan, Y. L. Ho, A. P. Lee. Droplet coalescence by geometrically mediated flow in microfluidic channels. Microfluid. & Nanofluid., 2007, 3, 495-499.
19. Y. C. Tan, J. S. Fisher, A. I. Lee, V. Cristini, A. P. Lee. Design of microfluidic channel geometries for the control of droplet volume, chemical concentration, and sorting, Lab. Chip., 2004, 4, 292-298.
20. L. H. Hung, K. M. Choi, W. Y. Tseng, Y. C. Tan, K. J. Shea, A. P. Lee. Alternating droplet generation and controlled dynamic droplet fusion in microfluidic device for CdS nanoparticle synthesis. Lab. Chip., 2006, 6, 174-178.
21. J. M. Kohler, T. Henkel, A. Grodrian, T. Kirner, M. Roth, K. Martin, J. Metze. Digital reaction technology by micro segmented flow—components, concepts and applications. Chem. Eng. J., 2004, 101, 201-216.
22. X. Niu, S. Gulati, J. B. Edel, A. J. de Mello. Pillar-induced droplet merging in microfluidic circuits. Lab. Chip., 2008, 8, 1837-1841.
23. D. E. Menech. Modeling of droplet breakup in a microfluidic T-shaped junction with a phase-field model. Phys. Rev. E, 2006, 73, 031505.
24. A. Carlson, M. Do-Quang, G. Amberg. Droplet dynamics in a bifurcating channel. Int. J. Multiphase Flow, 2010, 36, 397-405.
25. C. Chung, M. Lee, K. A. Char, K. H. Ahn, S. J. Lee, Droplet dynamics passing through obstructions in confined microchannel flow. Microfluid. & Nanofluid, 2010, 9, 1151-1163.
26. Y. Shi, G. H. Tang, H. H. Xia. Lattice Boltzmann simulation of droplet formation in T-junction and flow focusing devices. Computers & Fluids, 2014, 90, 155-163.
27. B. A. Nichita, I. Zun, J. R. Thome. A VOF method coupled with a dynamic contact angle model for simulation of two-phase flows with partial wetting. In: 7th Int. Conf. Multiphase Flow. 2010, Tampa, ICMF.
28. J. Lee, W. Lee, G. Son. Numerical study of droplet breakup and merging in a microfluidic channel. J. Mech. Sci. & Technol., 2013, 27, 6, 1693-1699.
29. S. L. Anna, N. Bontoux, H. A. Stone. Formation of dispersions using flow focusing in microchannels. Appl. Phys. Lett., 2003, 82, 364-366.
30. T Anna, T. Gun, T. Christian. CFD modelling of drop formation in a liquid-liquid system. In: 6th Int. Conf. Multiphase Flow. 2007, Leipzig, ICMF.
31. B. D. Hamlington, B. Steinhaus, J. J. Feng, D. Link, M. J. Shelley, A. Q. Shen. Liquid crystal droplet production in a microfluidic device. Liq. Cryst., 2007, 34, 861 870.
32. Q. S. Zou, X. Y. He. On pressure and velocity boundary conditions for the lattice Boltzmann BGK model. Phys. Fluids, 1997, 9, 1591-1598.
33. D. L. Youngs. Time-dependent multi-material flow with large fluid distortion. In: Numerical Methods for Fluid Dynamics. 1982, Wiley, 273-285.
34. M. Rudman. Volume-tracking methods for interfacial flow calculations. Int. J. Numer. Meth. Fluids, 1997, 24, 671-691.
35. D. A. Hoang, L. M. Portela, Ch. R. Kleijn. Numerical study on droplet breakup in a microfluidic T-junction. J. Fluid Mech. R, 2013, 717, 4, 1-11.
36. H. H. Liu, A. J. Valocchi, Q. J. Kang. Pore-scale simulation of high-density-ratio multiphase flows in porous media using lattice Boltzmann method. Comput. Phys., 2010, 229, 8045-8063.
37. W. Lee, G. Son. Numerical study of obstacle configuration for droplet splitting in a microchannel. Computers & Fluids, 2013, 84, 351-358.